Reviewing Image Enhancement Operators

Bernard Lampe, *Member, IEEE*

***Abstract*—This analysis will evaluate three types of digital image enhancement techniques commonly used in image processing. The first type is focused on global enhancement techniques which leverage the image intensity histogram while ignoring spatial correlations. Specifically, we explore histogram equalization and histogram specification using mixed Gaussian distributions to specify multi-modal models of the global histogram. The second set of techniques take advantage of the spatial correlation to improve image detail via sharpening. In particular, we will be examining unsharp masking and image high-boost filtering techniques. The final set are edge detection techniques which take advantage of spatial correlations and image contrast by exploiting spatial correlated gradients in the image intensities. In particular we are evaluating the classic Roberts, Sobel and Laplacian convolution operators. The analysis of each set of techniques will include cases in which the technique performs favorably resulting in image enhancement, has little effect resulting in no enhancement and fails resulting in image degradation. The discussion of each enhancement type will focus on the shortcomings of the techniques as exemplified in the failure cases. Finally, we do not put forth new metrics for evaluating the resulting image enhancements, but perform subjective assessments of processed images.**

***Index Terms*—Edge Detection, Enhancement, High-boost, Histogram**

I. Introduction

SIMPLE image processing operators are the foundation of any digital image analysis. In this paper we will explore fundamental image processing operators. The aim of this analysis has two goals. The first goal is to review classic image processing operators and identify the domain specific attributes which are exploited by these operators. The second goal is to empirically analyze images using these techniques and evaluate results. The discussion will focus on the limitation of these operators thereby suggesting proper application with other data sets.

Firstly, we focus on techniques which leverage the global image histogram. We utilize the histogram to compute discrete intensity mapping functions which are used to remap the intensity values from the original set to a set which has predefined properties. Two specific image processing techniques are explored. First is histogram equalization and the second is histogram specification. Histogram equalization is an automatic operator and requires only the original image as input to the process. However, histogram specification requires the input image as well as a probability mass function (PMF) which represents the resulting normalized histogram of the processed image. The implementation of histogram specification here uses mixtures of Gaussian PMF to specify the target histogram. The goal of both techniques is to compute an intensity mapping which will map the original image histogram to another with specified properties. [3, p. 120-138]

Secondly, we explore techniques which leverage spatial correlations by applying filters to emphasis high-frequency details via low-pass filtering and background subtraction. In particular, we examine unsharp masking and high-boost filtering. Both techniques perform estimation of the background via low-pass filter and then perform image subtraction. The subtracted images represent the result of a high-pass filter. These details are then scaled and added back to the original image to "boost" the high-frequency details. Finally, the image intensities are linearly remapped to the 8-bit range of (0-255). This results in image detail enhancement. [3, p. 162-165]

Finally, we examine techniques which leverage spatial correlation by applying multiple filters which compute image gradients of the first and second degree. By exploiting rapid intensity changes, these operators enhance image edge features. Specifically, we focus on the Robert cross and Sobel operators to compute first degree gradients and Laplacian operator to compute second degree gradient features. Each of these operators define normalized, filtering functions which compute spatially correlated image gradients. Finally, simple non-maximal suppression and thresholding algorithms are used to remove spurious gradient responses of low value. The resulting gradient functions represent spatial localities with rapid intensity changes indicative of edge features. [3, p. 165-172]

II. Methodology

A. Histogram Equalization

Histogram equalization is a global image processing operator that remaps the intensity values to improve image brightness in a way that is particularly suited to aid in human visual analysis. The goal is to produce an intensity mapping whereby the remapped image has an intensity histogram which is a scaled uniform distribution (all grey levels a equiprobable). [4, p. 75]

The histogram equalization mapping function is formed by computing the discrete cumulative distribution function (CDF) from the input image intensities. The CDF is then used as the intensity remapping function. The entire process is succinctly described in [3, p. 122-128] and is repeated here in equation 1.

$$s_k = T(r_k) = (L-1)\sum_{j=0}^{k} p_r(r_j) = \frac{(L-1)}{MN}\sum_{j=0}^{k} n_j \qquad k = 0, 1, 2, ..., L-1 \quad (1)$$

s_k	Transformed pixels of magnitude k
r_k	Original image pixels of magnitude k
T	Image pixel transform, in this case histogram equalization
L	Maximum magnitude of image pixel magnitude
p_r	Probability mass function
MN	Original image dimensions used to compute number of pixels
n_j	Count of pixels in original image of value j

TABLE I: Symbols Defined for Equation 1

B. Histogram Specification

Histogram specification is the generalization of the histogram equalization process. While histogram equalization imposes the constraint that the final histogram be a scaled uniform distribution function, histogram specification allows for an arbitrary specified histogram.

Histogram specification requires an input image as well as a specified PMF which is used to specify the desired histogram. The original image is first equalized using histogram equalization as in equation 1. Next, the specified PMF is used to compute a equalized mapping as in equation 2. Finally, the two mappings are seen as equivalent and the mapping computed from the specified PMF is inverted as in 3 thus providing a mapping from s_k to the final output z_q, thus producing the desired histogram. The implementation used in this paper uses Gaussian PMF mixtures to specify the desired histogram. The entire process is described in [3, p. 128-138] and is summarized in equations 1, 2, and 3.

$$G(z_q) = (L-1)\sum_{i=0}^{q} p_z(z_i) \tag{2}$$

$$z_q = G^{-1}(s_k) \tag{3}$$

$p_z(z_i)$	Specified PMF of pixel magnitude i
L	Maximum magnitude of image pixel magnitude
s_k	Transformed pixels of magnitude k from histogram equalization
z_q	Transformed pixels of magnitude q
G	Transform function computed from specified PMF

TABLE II: Symbol Defined for Equations 2 and 3

C. Unsharp Masking and High-Boost Filtering

Unsharp masking and high-boost filtering are global image processing operators that emphasize details in the image. The techniques are related in that they perform the same image processing operations. The amount of detail enhancement dictates which technique is being used. Emphasizing the details in unsharp masking uses the estimate of the high-frequency components directly, while high-boost filtering scales the high-frequency estimate before adding back to the original image.

Both operators follow the same process and are described here together. First, the low-frequency components of the input image are estimated by blurring the input using a spatial Gaussian function as a convolution function. Second, the blurred image is subtracted from the original resulting in an estimate of the high-frequency image components. Finally, the high-frequency estimate is added back to the original image and the image is linearly scaled to 8-bits (0-255). This process results in emphasizing the spatial correlations where-by the second derivatives have high values. The entire process is described in [3, p. 162-165] and is repeated here in equations 4 and 5 for convenience.

$$g_{mask}(x,y) = f(x,y) - \overline{f}(x,y) \tag{4}$$

$$g(x,y) = f(x,y) + k * g_{mask}(x,y) \tag{5}$$

$f(x,y)$	Original image function with spatial coordinates (x,y)
$\overline{f}$	Blurred image function estimating the background
$g_{mask}(x,y)$	Mask estimating the high-frequency image components
k	Specified scaling factor
$g(x,y)$	Final sharpened image

TABLE III: Symbol Defined for Equations 4 and 5

D. Edge Enhancement

Edge enhancement operators exploit spatial correlation of the image pixels by estimating the isotropic gradient to enhance edge features. The first-order gradient is estimated by approximating the orthogonal, component, first-order spatial derivatives of the image pixel magnitudes, and then computing the isotropic gradient vectors from the components. The gradient vector magnitudes are then thresholded to reduce false alarms by removing those gradients of low value. This process results in an image where the discontinuities in pixel magnitude are enhanced. The second-order spatial derivatives are estimated using a single isotropic filter that approximate the Laplacian function. Similar thresholding is performed on the second order gradient image to reduce false alarms.

The first-order edge enhancement operators explored here are the Robert cross and Sobel functions. The Robert cross function is a 2x2 mask used to estimate the first-order derivatives along the 45 and 135 degree vectors of the image basis via convolution in the spatial domain. The Sobel function is 3x3 mask used to estimate the first-order derivatives along the 0 and 90 degree vectors of the image basis via convolution in the spatial domain. Both of these operators were derived from the Taylor series function approximation as illustrated in equations 6 and 7. Both functions are pictured in figure 1. These orthogonal, component, gradient images are then used to compute the isotropic gradient magnitude as in equation 8. [4, p. 119-129]

$$f(x+\Delta x) = f(x) + \Delta x * f^{'}(x) + \frac{\Delta x^2}{2!} * f^{''}(x) + ... \tag{6}$$

$$f^{'}(x) = \frac{f(x+\Delta x) - f(x)}{\Delta x} \tag{7}$$

$$G(x,y) = \sqrt{G_1(x,y)^2 + G_2(x,y)^2} \tag{8}$$

The second-order edge enhancement operator examined here is the Laplacian function. The Laplacian function is a 3x3 mask used to estimate the second-order derivative using a single isotropic function. The Laplacian function is derived

+1	0
0	-1

(a) Roberts 1

0	+1
-1	0

(b) Roberts 2

1	0	-1
2	0	-2
1	0	-1

(c) Sobel 1

1	2	1
0	0	0
-1	-2	-1

(d) Sobel 2

0	-1	0
-1	4	-1
0	-1	0

(e) Laplacian

Fig. 1: Robert Cross, Sobel and Laplacian Filters

$G(x, y)$	Image gradient vector magnitude
$G_1(x, y)$	First component gradient of Robert cross or Sobel estimation
$G_2(x, y)$	Second component gradient of Robert cross or Sobel estimation

TABLE IV: Symbol Defined for Equations 8

from the difference in first order derivatives as illustrated in equation 9. The function is pictured in table 1. This function is convolved with this input image in the spatial domain producing a second-order gradient image that emphasizes spatially correlated, pixel magnitude discontinuities (i.e. zero-crossings). [4, p. 137-139]

$$f^{''}(x) \approx f^{'}(x) - f^{'}(x+1) \approx \\ - f(x) + 2f(x+1) - f(x+2) \quad (9)$$

III. Experiments

A. Experimental Image Data Set

The empirical analysis was performed on a classic image processing data set provided by Rafael C. Gonzalez to accompany his book [3]. We choose the classic images of Cameraman, House and Lena. Theses images were evaluated with each of the techniques. The set of three original images are pictured in figure 2.

(a) Cameraman (b) House (c) Lena

Fig. 2: Original images without processing

B. Histogram Equalization

We performed histogram equalization on each of the three images. The results of the processing are displayed in figures 3, 4, and 5.

The first case, Cameraman in figure 3, shows an increase in image contrast in the foreground and background. This technique has performed favorably on this image, resulting in high detail contrast. The buildings in the background are more visible and the details of the coat and camera are more pronounced. There is a slight increase in contrast of the noise in the background sky, but it does not obscure image details or cause objectionable artifacts.

(a) Cameraman Original (b) Cameraman Histogram Equalization

Fig. 3: Histogram Equalization of Cameraman

(a) Lena Original (b) Lena Histogram Equalization

Fig. 4: Histogram Equalization of Lena

(a) House Original (b) House Histogram Equalization

Fig. 5: Histogram Equalization of House

The second case, the Lena image in figure 4, shows a slight improvement in image contrast and brightness. This makes the image more pleasant to look at, but histogram equalization does not accent or emphasize any of the fine details. This image benefits from the technique, but shows little overall improvement due to the good quality of the original image.

The third case, the house image in figure 5, clearly shows that histogram equalization has failed at improving this image. The result of the technique shows objectionable artifacts in the background around the halo of the house. In addition, many of the fine details of the house have been destroyed due to the

spatially indiscriminate technique.

From this small empirical analysis we can see that histogram equalization can be a good technique, but suffers from draw backs if used without care. The problems with the technique are listed below.

1) Histogram equalization ignores spatial correlations in the image. This can result in background noise being enhanced and artifacts as seen in figure 5.
2) Histogram equalization may move objects in the background into the foreground.
3) Histogram equalization does not respect spatial correlation and will not preserve fine details present at edge boundaries.
4) Histogram equalization always sets the mean brightness of the image to 128 assuming an 8-bit image. This may not be the optimal brightness of an image.

C. Histogram Specification

We performed histogram specification on each of the three images. The results of the processing are displayed in figures 6, 8, and 10. In addition, the specified histograms were formed using a mixture of Gaussian PMFs. These functions are displayed in figures 7, 9, and 11.

(a) Cameraman Original (b) Cameraman Histogram Specification

Fig. 6: Histogram Specification of Cameraman

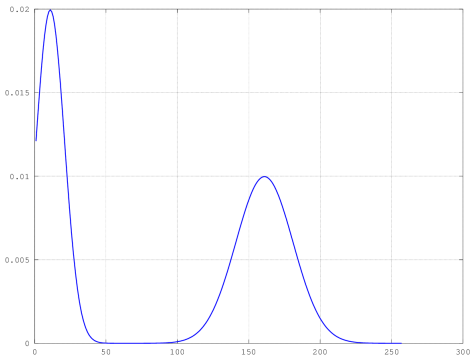

Fig. 7: Gaussian Mixtures used as Histogram Specifications for Cameraman

The first case, Cameraman in figures 6 and 7, shows a failure of this technique. Clearly the image has lost fine details and the background noise has increased in contrast

(a) Lena Original (b) Lena Histogram Specification

Fig. 8: Histogram Specification of Lena

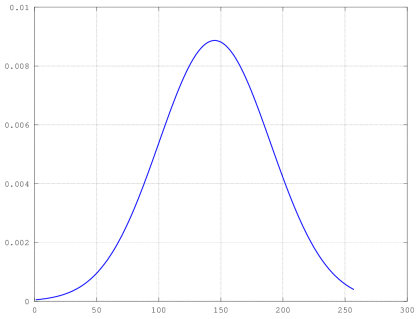

Fig. 9: Gaussian Mixtures used as Histogram Specifications for Lena

(a) House Original (b) House Histogram Specification

Fig. 10: Histogram Specification of House

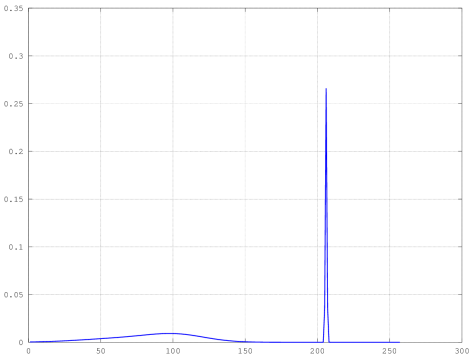

Fig. 11: Gaussian Mixtures used as Histogram Specifications for House

to an objectionable level. The failure of this technique was due to the limitations of the Gaussian mixture model used to approximate the specified histogram. As you can see in figure 7, the specified histogram used was a multi-model Gaussian PMF. This was chosen because it closely modeled the modes of the original image histogram. The attempt was to preserve the peaks of the original distribution. However, the failure is due to the reduced fidelity of the histogram. Mixtures of Gaussians PMFs were not adequate to provide a good model that would result in image enhancement.

The second case, Lena in figures 8 and 9, shows that the technique was ineffective on this image. There was no improvement, and very little degradation. The processed image shows little difference besides a slight decrease in brightness. The original image histogram was already very well modeled by a Gaussian distribution. Therefore, a single modal distribution was specified for processing and resulted in little effect.

The third case, House in figures 10 and 11, show much improvement over the histogram equalization technique. The specified histogram was empirically chosen to be multi-modal. The largest mode of the histogram models the background while the much smaller mode results in contrast stretching of the foreground. The resulting image is free of the artifacts that plagued the processing done with histogram equalization.

This small analysis shows that histogram specification is a powerful technique, but has shortcomings. The observed disadvantages of the technique are listed below.

1) Some histograms require complicated models that would be tedious or impossible to represent analytically. As seen in figure 6, the Gaussian mixtures do a poor job of modeling the optimal histogram resulting in image artifacts.
2) Histogram specification inherently ignores the spatial correlations, but this can be overcome if the foreground and background pixels are easily separable using the histogram.
3) Modeling of the specified histogram is not straight forward and requires trial-and-error.

D. Unsharp Masking and High-Boost Filtering

We performed High-Boost Filtering on each of the three images. The results of the processing are displayed in figures 12, 13, and 14.

The first case, Cameraman in figure 12, shows an adequate result from the high-boost filtering. While, the image details were clearly enhanced, some of the background noise was enhanced resulting in small artifacts throughout the image. This is especially apparent in the grass. The details of the grass do not require boosting, and certainly are degraded by the technique resulting in small artifacts.

The second case, Lena in figure 13, shows a very favorable result over the histogram equalization and histogram specification techniques. The fine details have been sharpened including very nice enhancement of the eyes, and mouth. In addition, the feather in her hat shows markedly more details. This technique outperforms both histogram based techniques previously applied because it accounts for spatial correlations.

(a) Cameraman Original (b) Cameraman High-Boost Filtering k = 14

Fig. 12: High-Boost Filtering of Cameraman

(a) Lena Original (b) Lena High-Boost Filtering k = 3

Fig. 13: High-Boost Filtering of Lena

(a) House Original (b) House High-Boost Filtering k = 5

Fig. 14: High-Boost Filtering of House

The histogram based techniques were ineffective because the original histogram already had good contrast and was well modeled by a Gaussian PMF.

The third case, House in figure 14, shows another adequate result. This image detail is clearly enhanced; however some of the noise in the shadows had been enhanced as well.

While this technique outperformed the histogram-based techniques with certain data, it cannot be used without care. Some of the observed disadvantages are listed below.

1) High-boost filtering takes into account spatial correlations, but is indiscriminate to what is in the image. For example, in figure 12, spurious details were enhanced resulting in artifacts.
2) Choosing the scaling factor is application specific and

subjective.

3) Images that were digitized via a scanner or other means may have lots of systematic noise that may be sharpened and result in artifacts.

E. Edge Enhancement Operators - Comparative Analysis

We performed edge enhancement of the Lena image as there are dominant high-frequency features in the feathered hat pictured. We computed the first order and second order gradient images and performed subsequent non-maximal suppression and thresholding to remove low magnitude gradients. The results of the processing are displayed in figures 15, 16, and 17.

(a) Lena Original (b) Lena Gradients using Robert Cross

Fig. 15: Component Gradients Computed via Robert Cross Operators

(a) Lena Original (b) Lena Gradients using Sobel Filters

Fig. 16: Component Gradients Computed via Sobel Operators

In the first case, using the Roberts cross filters in figure 15, we see that the edge features after thresholding the image gradients. Each of the thresholds was chosen by-hand for the three techniques used here. In addition, all thresholded images were subjected to non-maximal suppression to remove duplicate gradient responses. It is apparent that the Robert cross filters are sensitive to noise and have missed some edges. Most notably, the top of the hat. These edges had a small gradient magnitude and therefore were dismissed by the thresholding operation.

In the second case, using the Sobel filters in figure 16, we see that the edge features have been enhanced, but there is quite a bit more sensitivity to noise in the image. However, this technique did not miss many of the critical edges there were missed by the Roberts cross filters. This is due to the higher response of those edges to the Sobel filter. This cause them to persist in the presence of thresholding.

(a) Lena Original (b) Lena Zero-Crossings using Laplacian Filter

Fig. 17: Zero-Crossings Computed via Laplacian Filtering

In the third case, using the Laplacian filter in figure 17, we see that the edge features are enhanced, and there appear to be more critical edges detected than the Roberts cross filters, but less than the Sobel. However, the Laplacian technique appears to be more robust to noise than the Sobel technique.

When considering all three operators, the Laplacian appears to account for more spatial correlation due to the larger window size when compared to the Robert cross filters. In addition, the Laplacian appears to be less sensitive to noise than the Sobel operator. Finally, the Laplacian did miss some crucial edges when compared to the Sobel filters, but did out perform the Robert cross operators. The Robert cross filters missed more edges than the Laplacian. On this data set, the Laplacian performed the best by striking middle point between missed edges and noise response. However, this is subjective and can only be quantified in an actual application.

IV. Conclusion

Our review and analysis of fundamental image processing techniques has resulted in a list of shortcomings inherent in each of the techniques. These shortcomings serve as guiding principles when applying each of these techniques. Each technique was demonstrated in with standard data sets to both perform favorably and fail. Care must always be taken when applying these techniques and the user must have a deep understanding of his input data to ensure that the processed images are not degraded and usable signals are not compromised.

References

[1] D. H. Ballard and C. M. Brown. *Computer Vision*. Prentice-Hall, Englewood Cliffs, NJ, 1982.

[2] Rafael C. Gonzalez. Standard image processing test images. http://web.eecs.utk.edu/~gonzalez/ipweb2e/downloads/standard_test_images/, 2012. [Online; accessed 12-October-2012].

[3] Rafael C. Gonzalez and Richard E. Woods. *Digital Image Processing (3rd Edition)*. Prentice-Hall, Inc., Upper Saddle River, NJ, USA, 2006.

[4] Mark Nixon and Alberto S. Aguado. *Feature Extraction & Image Processing, Second Edition*. Academic Press, 2nd edition, 2008.

Bernard Lampe (M'09) became an IEEE Member (M) in 2009 and received his bachelors of science degree from The University of Michigan in Ann Arbor, Michigan, USA in 2009.

He served in the United States Air Force as a Staff Sergeant during the Iraq war from 1999-2005 supporting intelligence gathering efforts. After, he performed research and development on DARPA programs including fulfilling a critical role in the DARPA Visibuilding program phases. Currently, he is leading research in software vulnerability analysis for government customers in the Washington D.C region. His interests are primarily focused on remote sensing technologies in the RF modality especially on leveraging SAR imagery.

Mr. Lampe is also a member of the American Society for Computing Machines (ACM) since 2009.